

# Aharonov-Bohm oscillations in the local density of topological surface states

Zhen-Guo Fu,<sup>1,2</sup> Ping Zhang,<sup>2,3,\*</sup> and Shu-Shen Li<sup>1,†</sup>

<sup>1</sup>*State Key Laboratory for Superlattices and Microstructures, Institute of Semiconductors, Chinese Academy of Sciences, P. O. Box 912, Beijing 100083, People's Republic of China*

<sup>2</sup>*LCP, Institute of Applied Physics and Computational Mathematics, P.O. Box 8009, Beijing 100088, People's Republic of China*

<sup>3</sup>*Center for Applied Physics and Technology, Peking University, Beijing 100871, People's Republic of China*

We semiclassically study Aharonov-Bohm (AB) oscillations in the local density of states (LDOS) for topological insulator (TI) and conventional metal Au(111) surfaces with spin-orbit interaction, which can be probed by spin-polarized scanning tunneling microscope. Based on a general formula we obtain, which describes electron scattering with two impurities, we show that the AB oscillatory period of total LDOS is a flux  $\Phi_0=hc/e$  (weak localization) in both systems. Remarkably, an analogous weak antilocalization induced  $\Phi_0/2$  period in spin components of LDOS for TI surface is observed, while it is absent in Au(111). Our results reveal new unique quantum scattering phenomena occurred on TI surfaces.

PACS numbers: 73.20.At, 73.23.-b, 74.55.+v, 71.70.Eg

Spin-orbit interaction (SOI) variously existing in semiconductors [1] and metals [2] has been an active area of the modern condensed matter physics research, but especially, the topological insulators (TI), which has been detected in series of two-dimensional [3–5] and three-dimensional [6–11] materials, suggest new directions for this field since the strong SOI exists in TI. For straightforward reasons, weak antilocalization [12] arising from the SOI-induced Berry phase is expected to be observed in TI systems. Many efforts have been devoted to observing weak antilocalization in the HgTe quantum wells [13, 14], Bi<sub>2</sub>Te<sub>3</sub> [15–17], Bi<sub>2</sub>Se<sub>3</sub> [18–24], and other materials. Very recently, for example, in a transport experiment [18] of Bi<sub>2</sub>Se<sub>3</sub> nanowires, the Aharonov–Bohm (AB) oscillation with anomalous period  $\Phi_0=hc/e$  (twice the conventional period) of magnetoconductance was observed, while the weak antilocalization induced  $\Phi_0/2$  period was absent. The period of these oscillations in conductance is determined by the doping level and the disorder strength of the TI nanowire [19, 20]. In addition, an energy gap at Dirac cone opened by magnetic doping in TI films could also induce crossover from the weak antilocalization to the weak localization, which is tunable by the Fermi energy and the gap [25].

In this letter, for exploring weak antilocalization in topological surface state, we consider an imaginary AB interferometer consisting of a spin-polarized scanning tunneling microscope (SP-STM) tip and two identical nonmagnetic impurities apart tens nanometers on the TI surface as shown in the Fig. 1. When electrons travel along the clockwise and anticlockwise loops ( $\mathbf{r} \Rightarrow \mathbf{r}_1 \Rightarrow \mathbf{r}_2 \Rightarrow \mathbf{r}$ ) enclosing a finite area, the interference phenomena occur. The electron interference contribu-

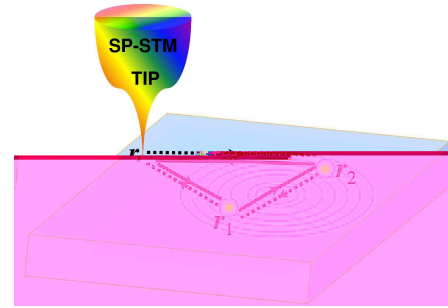


FIG. 1: (Color online) Surface electronic interferometer, comprising a spin polarized STM tip at  $\mathbf{r}$  and two impurities at  $\mathbf{r}_1$  and  $\mathbf{r}_2$  separately. The interference contributions in the LDOS is introduced by the electrons traveling along clockwise and anticlockwise loops enclosed by the STM tip and two impurities. The applied magnetic field affects this interference via the AB effect.

tions to the local density of states (LDOS) are affected by the magnetic field  $B$  via the AB effect arising from the phase (magnetic flux) difference between a path going clockwise and one going anticlockwise. We will show that, on one hand, the AB oscillatory period of total LDOS  $\Delta N_L^{\uparrow}(\mathbf{r}, \omega, B)$  (the subscription  $L$  represents the loops enclosed by the scattering paths of the surface electrons) is a flux  $\Phi_0$ , which is an analog of weak localization phenomenon. On the other hand, different from the spinless case [26], the strong SOI in TI materials can modify the electron AB interference effect via the spin rotations generated by the surface-electron noncollinear multiple scattering trajectories, and thereby the analogous weak antilocalization effect induced  $\Phi_0/2$  period in AB oscillations will be observed if the spin components ( $\Delta N_L^{\uparrow}(\mathbf{r}, \omega, B)$  and  $\Delta N_L^{\downarrow}(\mathbf{r}, \omega, B)$ ) are measured separately. Furthermore, for comparing with the results of TI surface, we briefly discuss the AB effect in the LDOS

\*zhang\_ping@iapcm.ac.cn

†slee@semi.ac.cn

of conventional metal Au(111) surface with weak SOI, and find that the analogous weak antilocalization phenomenon in the spin components is absent in Au(111) surface since the SOI is not sufficiently strong. This observation may provide a new method to character the topological surface states.

We describe the TI surface, on which two nonmagnetic impurities are adsorbed, by a low energy effective Dirac Hamiltonian written as

$$H = v\sigma \cdot (\hat{z} \times \mathbf{q}) + \sum_{i=1}^2 U_i \sigma_0 \delta(\mathbf{r} - \mathbf{r}_i) \quad (1)$$

with the Fermi velocity  $v=333$  (287) meV·nm in Bi<sub>2</sub>Se<sub>3</sub> (Bi<sub>2</sub>Te<sub>3</sub>) [28].  $\mathbf{q}=(q_x, q_y)$  denotes the planar momentum operator, and  $\sigma=(\sigma_1, \sigma_2, \sigma_3)$  is the Pauli spin matrix. The second term in this Hamiltonian represents the potential of two nonmagnetic impurities located at  $\mathbf{r}_1=(-d/2, 0)$  and  $\mathbf{r}_2=(d/2, 0)$  with strength  $U_i$ .  $\sigma_0$  is the  $2 \times 2$  unit matrix.

The features we discuss are expected to be seen in the change of the real space LDOS,  $\Delta N_L(\mathbf{r}, \omega, B)$ , owing to the influence of magnetic flux which passes through the area enclosed by the two scattering paths shown in Fig. 1. This quantity can directly reveal the weak (anti)localization effect in TI via AB oscillatory periods in LDOS. The real space Green's function involving the impurities scattering is given by Dyson equation  $G=G_0+\delta G$ , with

$$\delta G = \int d\mathbf{r}'' G_0(\mathbf{r} - \mathbf{r}''; \omega) V(\mathbf{r}'') G(\mathbf{r}'', \mathbf{r}'; \omega). \quad (2)$$

The bare electron Green's function  $G_0$  for the surface states of TI could be expressed in terms of a complex amplitude multiplied by a "complex" rotation:

$$G_0(\mathbf{r}, \mathbf{r}'; \omega) = \frac{|\omega^+|}{4v^2} D_+ \hat{R}(\alpha, \beta, \gamma), \quad (3)$$

which is useful to gain more physical insight into the transport between  $\mathbf{r}$  and  $\mathbf{r}'$ . Here,  $D_+=\sqrt{g_0^2+g_1^2}$ , where  $g_{0/1}=\text{sgn}(\omega^+) Y_{0/1}(|k|\rho) \mp i J_{0/1}(|k|\rho)$  with  $\rho=|\mathbf{r}-\mathbf{r}'|$ ,  $k=k_F(1+\omega/E_F)$ ,  $\omega^+=\omega+E_F$ , and  $E_F=vk_F$  the Fermi energy of TI.  $J_{0/1}$  ( $Y_{0/1}$ ) are the first (second) kind Bessel functions.  $\hat{R}(\alpha, \beta, \gamma)=e^{i\alpha\sigma_3} e^{i\beta\sigma_1} e^{i\gamma\sigma_3}$  is a spin rotation operator with the Euler angles  $\alpha=-\frac{\vartheta}{2}+\frac{\pi}{4}$ ,  $\beta=\tan^{-1}(\frac{g_1}{g_0})$ , and  $\gamma=-\alpha$ .  $\tan(\vartheta)=\frac{(\mathbf{r}-\mathbf{r}') \cdot \hat{y}}{(\mathbf{r}-\mathbf{r}') \cdot \hat{x}}$ . Equation (3) is exact under a high energy cutoff [27].

Following the perturbation approach, Eq. (2) can be expanded to any order in the impurity potential  $U_i$ . We just focus on the scattering processes of surface electrons with the both impurities, in which the scattering paths enclose loops. Therefore, taking all this into account, after a long algebra calculation, we have

$$\delta G_L = G_0(\mathbf{r} - \mathbf{r}_1) W_1 G_0(\mathbf{r}_1 - \mathbf{r}_2) T_2 G_0(\mathbf{r}_2 - \mathbf{r}') + G_0(\mathbf{r} - \mathbf{r}_2) W_2 G_0(\mathbf{r}_2 - \mathbf{r}_1) T_1 G_0(\mathbf{r}_1 - \mathbf{r}'), \quad (4)$$

where

$$W_{1/2} = \frac{T_{1/2}}{\sigma_0 - T_{1/2} G_0(\mathbf{r}_{1/2} - \mathbf{r}_{2/1}) T_{2/1} G_0(\mathbf{r}_{2/1} - \mathbf{r}_{1/2})} \quad (5)$$

is diagonal with  $T$ -matrices  $T_{1/2}=\frac{U_{1/2}}{1-U_{1/2}G_0(\mathbf{0};\omega)}\propto\sigma_0$ , and  $G_0(\mathbf{r}_1-\mathbf{r}_2)G_0(\mathbf{r}_2-\mathbf{r}_1)\propto\sigma_0$  since that there is no net spin rotation as electrons travel from  $\mathbf{r}_1$  to  $\mathbf{r}_2$  and then back to  $\mathbf{r}_1$ . Equation (4) is a general formula describing the interference effect from the scattering with both two impurities participated. In the absence of SOI, the two terms in Eq. (4), i.e., the scattering amplitudes corresponding to the time-reversal processes, should be equal to each other and thereby give rise to the constructive quantum correction to the LDOS in the so-called weak localization theory. In the presence of a strong SOI, however, the electrons interference is affected remarkably due to the noncollinear multiple scattering trajectories that generate nontrivial spin rotations. These spin rotations lead to a destructive interference in LDOS by a phase change picked up during the clockwise and anticlockwise scattering processes, which is the origin of the weak antilocalization in systems with strong SOI.

Applying a magnetic field tends to break the destructive interference and may give rise to some key signature of weak antilocalization effect, such as the AB oscillations with the expected  $\Phi_0/2$  period in spin components of LDOS (similar as  $\Phi_0/2$  period in magnetoconductivity due to weak antilocalization). In the presence of a low magnetic field, the Green's function can be semiclassically approximated as [29],

$$\tilde{G}_0(\mathbf{r} - \mathbf{r}') = \exp\left(i\frac{2\pi}{\Phi_0} \int_{\mathbf{r}}^{\mathbf{r}'} \mathbf{A}(\mathbf{l}) \cdot d\mathbf{l}\right) G_0(\mathbf{r} - \mathbf{r}'), \quad (6)$$

where  $\Phi_0=hc/e$  is the flux quantum, and  $\mathbf{A}=(-By, 0, 0)$  represents the vector potential. This approximation is exact so long as the magnetic length is much greater than the Fermi wave length ( $l_B=(\Phi_0/2\pi B)^{1/2} \gg \lambda_F$ ). For magnetic field  $B=5$  T $\sim$ 10 T, the corresponding magnetic length  $l_B \approx 11.63$  nm $\sim$ 8.22 nm, while the Fermi wave length  $\lambda_F=7.21$  nm $\sim$ 5.3 nm for TI within  $E_F=250$  meV $\sim$ 340 meV [7]. Accordingly, the condition in Eq. (6) for the semiclassical approximation is valid for these low magnetic field and low energy ranges.

The correction of the LDOS due to the magnetic flux is given by

$$\Delta N_L(\mathbf{r}, \omega, B) = -\frac{1}{\pi} \Im \text{Tr} \left[ \delta \tilde{G}_L(\mathbf{r}, \omega) - \delta G_L(\mathbf{r}, \omega) \right], \quad (7)$$

where  $\delta \tilde{G}_L$  is calculated from Eq. (4) with  $\tilde{G}_0$ . For large distances ( $|k|\rho \gg 1$ ),  $J_{0/1} \approx \pm \sqrt{2/(\pi|k|\rho)} \cos[\pi/4 \mp |k|\rho]$  and  $Y_{0/1} \approx \pm \sqrt{2/(\pi|k|\rho)} \sin[|k|\rho \mp \pi/4]$ . Combining Eqs.

(3-7), we get that

$$\begin{aligned} \Delta N_L(\mathbf{r}, \omega, B) &= \Delta N_L^\uparrow(\mathbf{r}, \omega, B) + \Delta N_L^\downarrow(\mathbf{r}, \omega, B) \\ &\approx C \Im[\tilde{t}(\omega) e^{i[\chi(r) - \pi/4]}] \left[ \cos\left(\frac{2\pi\Phi}{\Phi_0}\right) - 1 \right] \end{aligned} \quad (8)$$

with  $C \propto k^{-3/2} \sqrt{\frac{2}{d|\mathbf{r}-\mathbf{r}_1||\mathbf{r}-\mathbf{r}_2|}} \cos(\frac{\vartheta_2}{2}) \sin(\frac{\vartheta_1}{2}) \sin(\frac{\vartheta_1-\vartheta_2}{2})$ ,  $\tan(\vartheta_{1,2}) = \frac{(\mathbf{r}-\mathbf{r}_{1,2}) \cdot \hat{y}}{(\mathbf{r}-\mathbf{r}_{1,2}) \cdot \hat{x}}$ , and  $\chi(r) = k(d + |\mathbf{r}-\mathbf{r}_1| + |\mathbf{r}-\mathbf{r}_2|)$ . Here  $\tilde{t}(\omega) = \frac{t^2(\omega)}{1-t^2(\omega)[g_0^2(d)-g_1^2(d)]}$  with  $t(\omega) = \frac{U}{1-U \int \frac{d^2q}{(2\pi)^2} \frac{i\omega}{(i\omega)^2 - (vq)^2}}$  is the nontrivial element of  $T$ -matrix. One can notice that  $[g_0^2(d) - g_1^2(d)]$  vanishes within the above asymptotic representation of  $J_{0/1}$  and  $Y_{0/1}$ .

Obviously, the AB oscillations arise from the factor  $\cos(\frac{2\pi\Phi}{\Phi_0})$  in Eq. (8), and the oscillation period is  $\Phi_0 = hc/e$ , resulting in weak localization effect in total LDOS, which is a direct consequence of the semiclassical approximation in Eq. (6). Correspondingly, to observe a complete AB oscillation period in the total LDOS  $\Delta N_L(\mathbf{r}, \omega, B)$  pattern in real space, the magnetic field should satisfy the relation that

$$B_{2\pi} \sim 2\Phi_0/yd. \quad (9)$$

Now let us analyze the spin-up and spin-down components of LDOS. The unique strong SOI nature of TI affects the surface electron interference due to the non-collinear multiple scattering trajectories that generate nontrivial spin rotations, which can be easily obtained by the rotation operator  $\hat{R}(\alpha, \beta, \gamma)$  in the Green's function  $G_0$  in Eq. (3). Explicitly, the AB oscillations of spin components of LDOS are given by

$$\begin{aligned} \Delta N_L^{\uparrow/\downarrow}(\mathbf{r}, \omega, B) &= \frac{C}{2} \Im[\tilde{t}(\omega) e^{i[\chi(r) \pm \pi/4]}] \\ &\times \left[ \sqrt{2} \frac{\sin(\phi \mp \frac{\pi}{4})}{\sin(\phi)} \cos\left(\frac{2\pi\Phi}{\Phi_0}\right) - 1 \right]. \end{aligned} \quad (10)$$

where  $\phi = (\vartheta_1 - \vartheta_2)/2$ . As clearly seen from this equation, comparing to the total LDOS, there occur in the spin-resolved LDOS additional phase factors  $\sin(\phi \mp \frac{\pi}{4})/\sin(\phi)$ , which arise from spin rotation during electron loop-traveling processes. These factors modulate the AB oscillatory period in the spin components of LDOS, so as to vary from the  $\Phi_0$  period of total LDOS, and hereby we expect that an analog of weak antilocalization induced  $\Phi_0/2$  period phenomenon can be observed in the AB oscillations of the spin-polarized LDOS in TI [see the following numerical results shown in Fig. 2 (b) and 2(c) below].

Moreover, the interference signature of LDOS decays by a factor of  $[d|\mathbf{r}-\mathbf{r}_1||\mathbf{r}-\mathbf{r}_2|]^{-1/2}$  in the asymptotic representation, Eqs. (8) and (10). Actually, however, dephasing processes have been observed in transport investigations in  $\text{Bi}_2\text{Se}_3$  and  $\text{Bi}_2\text{Te}_3$  films [16, 22–24] as well

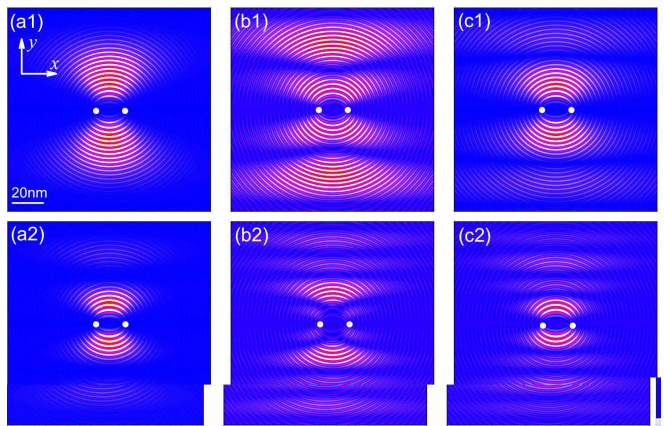


FIG. 2: (Color online) Simulations of the AB oscillations of the electronic LDOS in  $\text{Bi}_2\text{Te}_3(111)$  surface with fixed magnetic field  $B=5$  T (upper panels) and  $B=10$  T (lower panels). (a) the total LDOS patterns; (b) the spin-up component; (c) the spin-down component. The parameters are chosen as  $v=287$  meV·nm,  $E_F=250$  meV ( $\lambda_F=7.21$  nm) and  $d=20$  nm. The white dots denote the positions of adatoms.

as in AB-effect studies of  $\text{Bi}_2\text{Se}_3$  nanowires [18–20]. The phase coherence length  $l_\phi$  of  $\text{Bi}_2\text{Se}_3$  and  $\text{Bi}_2\text{Te}_3$  can be as large as hundreds of nanometers, which is tens times of the Fermi wave length. The characteristic distance in our setup must be much smaller than the phase coherence length ( $d \leq l_\phi$ ) [26], so that we choose  $d=20\text{nm} \ll l_\phi$  without taking into account the dephasing processes in the following numerical calculations.

To supplement the above analytical results, we give the typical numerically calculated data in Fig. 2, where the upper (lower) panels correspond to  $B=5$  T (10 T). The blue horizontal strips are the AB oscillation signals in the real-space LDOS, while the oscillatory ellipse features are the interference signals arising from the contributions of  $N_L(\mathbf{r}, \omega, B=0)$ . It is obvious that in the case of  $B=5$  T (10 T), the interval between the nearest-neighbor oscillation strips is  $y \approx 85$  nm (42 nm) in the total LDOS as shown in Fig. 2 (a), corresponding to the  $\Phi_0$  period of AB oscillations as analytical calculations show above.

However, differing from the AB oscillations in the total LDOS, in the case of  $B=5$  T (10 T) the interval between the nearest-neighbor oscillation strips becomes  $y \approx 42$  nm (21 nm) in the spin-up and spin-down components, which is a half of the oscillatory period of the total LDOS, as illustrated in Figs. 2(b) and 2(c) [30]. This is an analogous phenomenon of weak antilocalization with a period of  $\Phi_0/2$  in spin components because of the strong SOI, which is within our expectation in above analytical discussions. Because of the existence of strong SOI in TI materials, a weak antilocalization phenomenon should be naturally observed in the spin components of LDOS in SP-STM experiments. This can be understood with Berry phase. Similar as the Berry phase of  $\pi$  induced by the  $2\pi$  rotation of

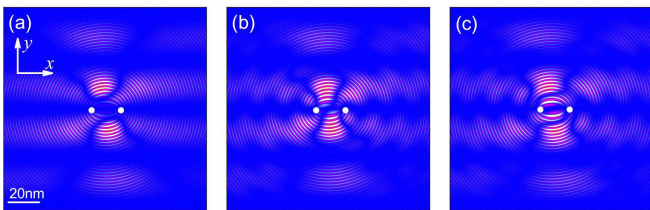


FIG. 3: (Color online) Simulated STM maps of the AB oscillations of the LDOS for two identical impurities 20 nm apart on the Au(111) surface with a SOI constant  $\gamma=40$  meV-nm under  $B=10$  T. (a) the total LDOS pattern, (b) and (c) the spin-up and spin-down components, separately. The effective electron mass  $m^*=0.26m_0$  and the Fermi wave length  $\lambda_F=3.74$  nm have been chosen.

the spin as it circles around the cylindrical surface of TI nanowires [19, 20], a corresponding Berry phase of each trajectory in our AB interferometer could be introduced:  $\Delta\varphi = -i \int_0^T dt \langle \psi_s(q_t) | \frac{\partial}{\partial t} | \psi_s(q_t) \rangle = s\pi$  ( $s=\pm 1$ ), where  $\psi_s(q) = \frac{1}{\sqrt{2}} (se^{i\theta(q)}, 1)^T$  is the eigenstate of free Hamiltonian of TI surface with  $\tan[\theta(q)] = \frac{q_y}{q_x}$ . This Berry phase of  $\pi$  suppress the backscattering in momentum space, and can lead to weak antilocalization effect in the spin components of LDOS of TI, which can be observed from the AB oscillations in the spin-resolved LDOS in the present interferometer. The key requirements for observing this effect are SP-STM tip and sufficient strong scattering potentials, which we believe are achievable in current experimental capabilities.

For comparison, we also calculate the AB oscillations on the conventional metal surface with weak but observable SOI. We choose Au(111) as an example, in which the Rashba SOI is  $\sim 40$  meV-nm and the Fermi wave

length is  $\sim 3.74$  nm [31]. The consequent calculated results are shown in Fig. 3 for  $B=10$  T. From Fig. 3 the SOI influence on electron interference in Au(111) can be summarized as follows: (i) The AB oscillation strips in the spin-split LDOS display oscillation behavior along  $x$  axis, which is caused by the spin rotations induced by noncollinear multiple scattering trajectories; (ii) The SOI destroys the elliptic features in the LDOS maps even if there is no applied magnetic field, see the *longitudinal* extending blue strips in Fig. 3. However, the AB oscillation period in the LDOS patterns is also  $\Phi_0$  (the interval between the nearest-neighbor horizontal blue strips is  $y \approx 42$  nm); (iii) Especially, there is no  $\Phi_0/2$  period in the spin-split LDOS in Fig. 3, which is totally different from the case of TI surface.

In summary, we have performed a semiclassical analysis of the SP-STM probed AB oscillations in the LDOS induced by two impurities on a TI surface as well as on a conventional metal surface with spin splitting. We have found that the total LDOS in both systems present weak localization phenomenon with an oscillatory period  $\Phi_0$  in the AB oscillations. Remarkably, the analogous weak antilocalization signified by a  $\Phi_0/2$  oscillation period has been found in the spin-split LDOS in the TI system, while it was absent in the conventional metal surfaces. This phenomenon, which can be observed in the SP-STM experiments, may provide an important signature for the existence of the topological surface states and provide a new criterion to distinguish the TI surface from other two-dimensional systems.

This work was supported by NSFC under Grants No. 90921003, No. 60776063, and No. 60821061, and by the National Basic Research Program of China (973 Program) under Grants No. 2009CB929103 and No. G2009CB929300.

- 
- [1] Y. A. Bychkov *et al.*, J. Phys. C **17**, 6039 (1984).  
[2] S. LaShell *et al.*, Phys. Rev. Lett. **77**, 3419 (1996).  
[3] C. L. Kane *et al.*, Phys. Rev. Lett. **95**, 226801 (2005).  
[4] B. A. Bernevig *et al.*, Science **314**, 1757 (2006); B. A. Bernevig *et al.*, Phys. Rev. Lett. **96**, 106802 (2006).  
[5] M. König *et al.*, Science **318**, 766 (2007).  
[6] L. Fu *et al.*, Phys. Rev. Lett. **98**, 106803 (2007).  
[7] Y. L. Chen *et al.*, Science **325**, 178 (2009).  
[8] D. Hsieh *et al.*, Nature **452**, 970 (2008); D. Hsieh *et al.*, Phys. Rev. Lett. **103**, 146401 (2009).  
[9] Y. Xia *et al.*, Nature Phys. **5**, 398 (2009).  
[10] J. E. Moore *et al.*, Phys. Rev. B **75**, 121306(R) (2007).  
[11] H. Zhang *et al.*, Nature Phys. **5**, 438 (2009).  
[12] G. Bergmann, Solid State Comm. **42**, 815 (1982).  
[13] E. B. Olshanetsky *et al.*, JETP Lett. **91**, 347 (2010).  
[14] G. Tkachov *et al.*, arXiv:1102.4512v1 (2011).  
[15] M. Z. Hasan *et al.*, arXiv:0912.5046v1 (2009).  
[16] H.-T. He *et al.*, arXiv:1008.0141 (2010).  
[17] P. Ghaemi *et al.*, Phys. Rev. Lett. **105**, 166603 (2010).  
[18] H. Peng *et al.*, Nature Mater. **9**, 225 (2010).  
[19] J. H. Bardarson *et al.*, Phys. Rev. Lett. **105**, 156803 (2010).  
[20] Y. Zhang *et al.*, Phys. Rev. Lett. **105**, 206601 (2010).  
[21] I. Chen *et al.*, Phys. Rev. Lett. **105**, 176602 (2010).  
[22] J. G. Checkelsky *et al.*, arXiv: 1003.3883v1 (2010).  
[23] M. Liu *et al.*, arXiv:1011.1055 (2010).  
[24] J. Wang *et al.*, arXiv:1012.0271v1 (2010).  
[25] H.-Z. Lu *et al.*, arXiv:1101.5437v1 (2011).  
[26] A. Cano *et al.*, Phys. Rev. B **80**, 153401 (2009).  
[27] R. R. Biswas *et al.*, Phys. Rev. B **81**, 233405 (2010).  
[28] C.-X. Liu *et al.*, Phys. Rev. B **82**, 045122 (2010).  
[29] B. L. Altshuler, *et al.*, Phys. Rev. B **22**, 5142 (1980).  
[30] To be more precise, the AB oscillations for the two spin components of LDOS have different phase shifts [see Eq. (10)] so that those oscillatory strips located at  $y \sim \pm(2n+1) \times 21$  nm ( $n$  is an arbitrary positive integer) are washed out but others at  $y \sim \pm 2n \times 21$  nm in the LDOS patterns of spin components are saved in the total LDOS with a  $\Phi_0$  period.  
[31] J. D. Walls *et al.*, Nano Lett. **7**, 3377 (2007).